Oceanologia (2017) 59, 445—459

Available online at www.sciencedirect.com

ScienceDirect

journal homepage: www.journals.elsevier.com/oceanologia/

ORIGINAL RESEARCH ARTICLE

Monthly dynamics of carbon dioxide exchange across the sea surface of the Arctic Ocean in response to changes in gas transfer velocity and partial pressure of CO_2 in 2010

Iwona Wrobel *

Institute of Oceanology, Polish Academy of Sciences, Sopot, Poland

Received 5 July 2016; accepted 17 May 2017
Available online 7 June 2017

KEYWORDS
Partial pressure of CO_2;
Gas transfer velocity;
Arctic fjord;
Air—sea CO_2 fluxes;
Greenland and Barents seas

Summary The Arctic Ocean (AO) is an important basin for global oceanic carbon dioxide (CO_2) uptake, but the mechanisms controlling air—sea gas fluxes are not fully understood, especially over short and long timescales. The oceanic sink of CO_2 is an important part of the global carbon budget. Previous studies have shown that in the AO differences in the partial pressure of CO_2 (ΔpCO_2) and gas transfer velocity (k) both contribute significantly to interannual air—sea CO_2 flux variability, but that k is unimportant for multidecadal variability. This study combined Earth Observation (EO) data collected in 2010 with the in situ pCO_2 dataset from Takahashi et al. (2009) (T09) using a recently developed software toolbox called FluxEngine to determine the importance of k and ΔpCO_2 on CO_2 budgets in two regions of the AO — the Greenland Sea (GS) and the Barents Sea (BS) with their continental margins. Results from the study indicate that the variability in wind speed and, hence, the gas transfer velocity, generally play a major role in determining the temporal variability of CO_2 uptake, while variability in monthly ΔpCO_2 plays a major role spatially, with some exceptions.

* Correspondence address: Institute of Oceanology Polish Academy of Sciences,Powstańców Warszawy 55, 81-712 Sopot, Poland. Tel.: +48 587311801.
E-mail address: iwrobel@iopan.gda.pl.
Peer review under the responsibility of Institute of Oceanology of the Polish Academy of Sciences.

Production and hosting by Elsevier

http://dx.doi.org/10.1016/j.oceano.2017.05.001

1. Introduction

The global carbon cycle plays an important role in energy and mass exchange in the Earth System and links the components of this system (land, ocean, atmosphere) (Garbe et al., 2014; Thomas et al., 2004). Increases in atmospheric carbon dioxide (CO_2) concentrations caused mainly by the burning fossil fuels, cement production and growing urbanization are directly responsible for 60% of the average global air temperature increase (IPCC, 2013; Kulinski and Pempkowiak, 2011). Half of the CO_2 emitted remains in the atmosphere while the rest is absorbed by the oceans and land biomass (Le Quéré et al., 2010, 2016; Omar et al., 2003; Sabine et al., 2004; Yasunaka et al., 2016). Relevant knowledge of air–sea CO_2 fluxes and their spatial and temporal variability is essential to gain the necessary understanding of the global carbon cycle and to fully resolve the ocean's role in climate variability (Le Quéré et al., 2013; Wanninkhof et al., 2009; Woolf et al., 2013). It is well known that the Arctic Ocean (AO) is an overall sink for CO_2 throughout the year even though continental shelves can either be regional or seasonal sinks or sources of atmospheric CO_2. However, there is a lot of uncertainty in calculating the CO_2 budgets of marginal and coastal shelf seas especially in the Polar Ocean margins (Cai et al., 2006; Doney et al., 2009; Landschützer et al., 2014). At present, the net air–sea CO_2 fluxes in the AO have been estimated at -0.12 ± 0.06 PgC yr^{-1} with net global ocean CO_2 uptake at -2.2 ± 0.5 PgC yr^{-1} (Goddijn-Murphy et al., 2015; Gruber, 2009; Schuster et al., 2013; Takahashi et al., 2009; Wanninkhof et al., 2013). Additionally, Cai et al. (2006) have shown that the average sea–air CO_2 flux for Arctic shelves is estimated as -12 ± 4 gC m^{-1} a^{-1}. Arctic shelves are greatly influenced by sea ice cover and the age of terrestrial inputs resulting in large CO_2 sinks during ice-free periods (Bates and Mathis, 2009; Cai et al., 2006).

Projections of trends in net carbon dioxide air–sea fluxes suggest that, in the future, CO_2 uptake by the ocean will increase because of sea ice loss (IPCC, 2013; Rödenbeck, 2005; Schuster et al., 2013). Reports have also been published, indicating that the seawater partial pressure of CO_2 (pCO_{2W}) in the North Atlantic has increased at a rate higher than the atmospheric pCO_2 (pCO_{2A}) (Lefèvre et al., 2004; Olsen et al., 2003).

Currently, there are several different approaches for estimating air–sea CO_2 fluxes. The first involves measuring direct fluxes using eddy correlation techniques (Else et al., 2011; Kondo and Tsukamoto, 2012; Repina et al., 2007). Another method focuses on calculating net air–sea CO_2 exchange with a mass balance assessment of carbon stocks and the inputs/outputs of carbon or vertical variations in DIC (Dissolved Inorganic Carbon) (Arrigo et al., 2010; MacGilchrist et al., 2014). The third approach takes into account differences in atmospheric and seawater pCO_2 combined with gas transfer velocity parameterizations (k) (Bates and Mathis, 2009; Boutin et al., 2002; Land et al., 2013; Landschützer et al., 2014; Takahashi et al., 2009). This final approach can employ the neural network technique, the advantage of which is that it can "notice" and exploit unpredicted correlations in the data (Lefèvre et al., 2005; Telszewski et al., 2009; Yasunaka et al., 2016).

In this article, the net CO_2 flux across the sea surface is calculated by multiplying ΔpCO_2 by the CO_2 gas transfer velocity coefficient (k), which depends primarily on the degree of turbulence near the interface. The direction and rates of net air–sea CO_2 exchange are determined by the product of the difference in values between pCO_2 in seawater and the atmosphere, and also by the rate of k. Positive ΔpCO_2 values indicate that the sea is a source of atmospheric carbon dioxide, whereas negative values indicate that it is a sink. Choosing the appropriate formula for gas transfer velocity is the key when calculating net air–sea gas fluxes. The main difficulty in quantifying k is its dependence on several physicochemical elements of the environment, such as surfactants, wind speed, sea state, surface roughness and breaking waves (Ho et al., 2006; McGillis et al., 2001; Shutler et al., 2016; Takahashi et al., 2009; Wanninkhof et al., 2009). In the literature, a wide range of different gas transfer parameterizations can be found that were derived using a number of techniques, e.g., Wanninkhof and McGillis (1999), Nightingale et al. (2000), McGillis et al. (2001), Ho et al. (2006), and Wanninkhof et al. (2013). At present, parameterizations with a quadratic wind speed relationship are interchangeable in the Arctic as Wrobel and Piskozub (2016) have shown. Fluxes resulting from using these functions (Ho et al., 2006; Wanninkhof et al., 2013) are only 3–4% higher (Fig. 1), respectively, than the most accurate parameterization applied to the study region, which is Nightingale et al. (2000) (see also Wrobel and Piskozub, 2016). Earlier studies showed that over interannual and shorter timescales, both components of the right hand side of Eq. (1) are significant in controlling air–sea fluxes, with only a few exceptions (Couldrey et al., 2016; Doney et al., 2009). Over longer, interannual to multidecadal timescales, flux variability is controlled only by ΔpCO_2 (Bates, 2012; Couldrey et al., 2016; Doney et al., 2009; Gruber et al., 2003; Le Quéré et al., 2000). The high uncertainty in the size of the net AO sink stems from the lack of coordinated in situ measurements in the winter; data are interpolated for the rest of the year. A potential alternative solution lies in exploiting satellite data from EO techniques (Boutin et al., 2002).

When studying air–sea CO_2 exchange across the sea surface in the AO, one has to remember the important role of extensive ice coverage in this process. Because of this, the monthly dynamics of air–sea interactions were analyzed in this paper during a one year period. Seasonal sea ice cover can reduce the exchange of CO_2 across the sea surface, but it

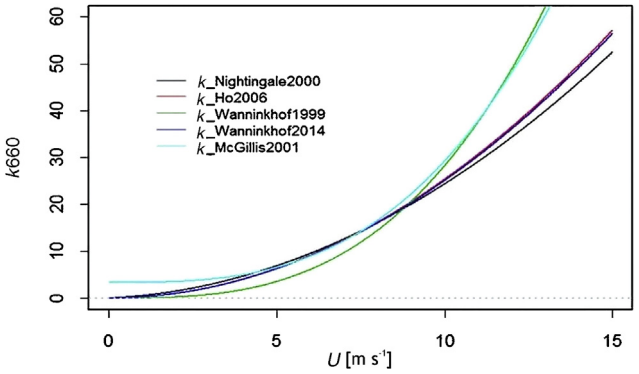

Figure 1 Gas transfer velocity [m s^{-1}] using different parameterizations as a function of wind speed [m s^{-1}].

also influences biogeochemical processes in surface water, especially inside Arctic fjords. The decrease of sea ice cover can result in an increase in outgassing in shallow shelf areas when surface waters are mixed deeper during the spring and winter. As was demonstrated in earlier studies by Olsen et al. (2003), Arrigo et al. (2008), Sejr et al. (2011), and others, sea ice loss in the AO produces a large area of open, ice-free water that is favorable for phytoplankton growth. Thinner seasonal sea ice cover replaces thick multi-year sea ice which makes it a weaker barrier for sea ice exchange, which means that phytoplankton spring blooms can absorb more CO_2 (Arrigo et al., 2008). Decreases of sea ice extent also cause water surface warming and, thus, act to reduce the CO_2 uptake by the ocean (Bates and Mathis, 2009). We do not yet fully understand whether decreased sea ice extent will indirectly affect higher CO_2 uptake by the ocean in the Arctic or not.

Trends and variability in the Arctic CO_2 sink have been studied intensively. Observations suggest its decrease is caused by increased in-water pCO_2 (Ashton et al., 2016; Boutin et al., 2002; Goddijn-Murphy et al., 2016; Lefèvre et al., 2004; MacGilchrist et al., 2014; Schuster et al., 2013). Marine pCO_2 seems to have been rising faster than atmospheric pCO_2, especially in the summer (Couldrey et al., 2016). The results from the FluxEngine-based Earth Observation (EO) data obtained from the European Space Agency OceanFlux Greenhouse Gases (GHG) Evolution project (http://www.oceanflux-ghg.org/) to evaluate how flux variability is controlled on short timescales. The present study examines the following testable hypothesis: air–sea CO_2 fluxes on a one year timeframe are dependent on both ΔpCO_2 and k.

1.1. Study area

The AO (Fig. 2) is relatively small ($\sim 10.7 \times 10^6$ km), and belongs to a class of ocean basins known as Mediterranean seas, with broad, shallow (<200 m deep) continental shelves surrounding a central basin. The AO has limited pathways of communication with Atlantic and Pacific waters, through the Bering Strait, the Canadian Archipelago, the Fram Strait and the Norwegian Sea gateways. Thermohaline forcing is the dominant driver (Piechura and Walczowski, 2009). Seasonal sea ice cover, especially in winter, reduces the exchange of energy, mass, and gases between the atmosphere and the ocean, and it also has a negative effect on sunlight penetration into the ocean that is needed for photosynthesis. Whether the Arctic acts as a sink or a source of CO_2 is controlled by many variables that are, themselves, influenced by climate change, including biological activity (Arrigo et al., 2010), temperature (Polyakov et al., 2004), riverine inputs (Dai et al., 2009), and sea ice melt (Bates and Mathis, 2009).

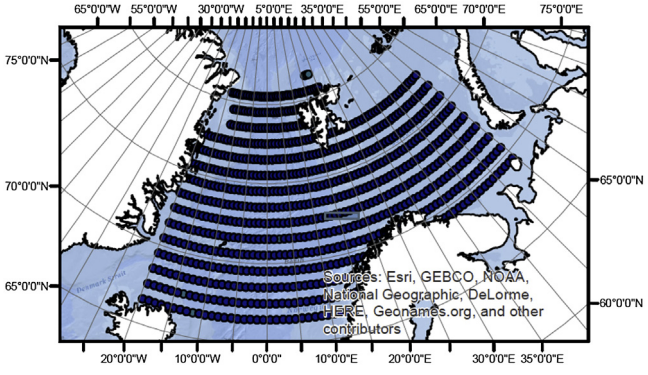

Figure 2 Study area (source: ArcGis basemap) — Greenland Sea and Barents Sea with sampling points.

The Barents Sea (BS) is the largest of the AO seas (1,424,000 km^2 area with a volume of about 316,000 km^3) and covers broad, shallow continental shelves with a maximum depth of ~600 m (average depth ~229 m) (Gurgul, 2002). It is characterized by an inflow of warm, saline Atlantic water via the Norwegian Atlantic Current and minimal freshwater inputs (Omar et al., 2003). Maximum wind speeds over the BS are about 20 m s^{-1}, with an average of approximately 6 m s^{-1} (Gurgul, 2002). Warm, saline Atlantic water is transformed into subsurface water by the process of brine rejection from sea ice formation or the cooling of surface water, and it is then transported to the Kara Sea and the central basin of the AO (Omar et al., 2007).

The Greenland Sea (GS) covers an area of 1,205,000 km^2 with an average depth of 1450 m and a maximum depth of approximately 5500 m. It lies south of the Arctic Basin and is a major pathway for the exchange of Arctic water with warm, saline Atlantic water through the Fram Strait via the deep East Greenland Current. Greenland Sea Deep Water is formed in the central GS, and it aerates the North Atlantic Deep Water (Nakaoko et al., 2006).

2. Methods

2.1. Data sets

Net air–sea CO_2 fluxes were calculated using the FluxEngine toolset (Shutler et al., 2016), which was created as a part of the European Space Agency funded OceanFlux Greenhouse Gases project (http://www.oceanflux-ghg.org) to encourage the use of satellite Earth Observation data. The toolbox allows its users to create their own climatology from the data available. After choosing the relevant data and formulae, users can create monthly global flux datasets. FluxEngine is available publicly on the Ifremer/CERSAT (Centre d'Exploitation et de Recherche Satellitaire) Nephelae Cloud (no specific skills are required to use it), and can be run through a web interface (http://cersat.ifremer.fr/data/collections/oceanflux) or it can also be downloaded. The source code can be downloaded from a GitHub server (Goddijn-Murphy et al., 2015; Shutler et al., 2016; Wrobel and Piskozub, 2016).

The calculations for this study were based on the climatological mean distribution of surface water pCO_2 and salinity values from Takahashi et al. (2009) (T09) climatology, archived at the Carbon Dioxide Information and Analysis Centre (CDIAC, Oak Ride, National Laboratory (Takahashi et al., 2008)) in non-El Niño conditions. T09 data were normalized to 2010 to evaluate seasonal variations in air–sea CO_2 fluxes (the calculations were based on Olsen et al. (2003), Omar et al. (2003), Nakaoko et al. (2006), Goddijn-Murphy et al. (2015) approaches, that assumed the partial CO_2 pressure in seawater has increased at a rate of 1.5 μatm yr^{-1}, on average observed for CO_2 partial pressure

in the air). Wind speed data at 10 m a.s.l. were obtained from the GlobWave project (http://globwave.ifremer.fr/), which produced a 20-plus year time series of global coverage multi-sensor cross-calibrated wave and wind data. The Sea Surface Temperature (SST) data were obtained from Ifremer/CERSAT and produced OceanFlux from ARC/(A)ATRS (Advance Along Track Scanning Radiometer measurements) carried out by the Envisat satellite (Merchant et al., 2012). SST_{skin} data are defined as the *"radiometric temperature of the surface measured by an infrared radiometer operating in the 1–12 μm waveband (10–20 μm depth"* according to definition in The Global Ocean Data Assimilation Experiment (GODAE) high-resolution sea surface temperature pilot project; Minnett and Kaiser-Weiss, 2012). The (A)ATSR is a self-calibrating radiometer that provides estimates of SST and exhibits a very small standard deviation of error. The k coefficient was estimated using the Nightingale et al. (2000) parameterization (hereafter called N2000, Fig. 1), which best fits the AO (Wrobel and Piskozub, 2016). All input data and climatologies were linearly re-interpolated to a $1^\circ \times 1^\circ$ geographical grid from the original resolution, and calculated for 2010 using the FluxEngine toolset. Data were extracted for the AO (north of 66°) from global resolution.

2.2. Parameterizations

The air–sea CO_2 flux is controlled by wind speed, SST, Sea Surface Salinity (SSS), sea state, and biological activity (Goddijn-Murphy et al., 2016). The calculations of CO_2 flux between the air and the sea [F, mgC m^{-2} day^{-1}] are given based the ΔpCO_2 [μatm] across a thin (~10–250 μm) mass boundary layer at the sea surface and the solubility of CO_2 [α, g m^{-3} μatm^{-1}] multiplied by the gas transfer velocity [k, cm h^{-1}] as a function of wind speed. The concentration of CO_2 in the sea water is a function of SSS and SST, its solubility [α, g m^{-3} μatm^{-1}], and its fugacity [fCO_2, μatm]. Hence, the standard bulk formula for the flux (F) was defined as:

$$F = k(\alpha_W pCO_{2W} - \alpha_S pCO_{2A}), \quad (1)$$

where S is the air–sea interface, A is the air, and W is water. We can replace fugacity with partial pressure (their values differ by $< 0.5\%$ over the temperature range considered) (McGillis et al., 2001). So Eq. (1) becomes:

$$F = k(\alpha_W pCO_{2W} - \alpha_S pCO_{2A}), \quad (2)$$

$$F = k\alpha\Delta pCO_2. \quad (3)$$

Gas transfer velocity was mainly parametrized as:

$$k_W = Sc^{-n}(a_0 + a_1 U + a_2 U^2 + a_3 U^3), \quad (4)$$

(Wanninkhof et al., 2009) where ($a_0 \ldots a_n$) are coefficients (one or more of which may be set to zero) of polynomials in wind-speed U [m s^{-1}], Sc is the Schmidt number of dissolved gas. Schmidt numbers at the skin surface (Sc_{skin}) are a function of SST [= (kinematic viscosity of water)/(diffusion coefficient of CO_2 in water)]. The Schmidt number for CO_2 in seawater at 20°C is equal to 660.0. The calculations were based on the Nightingale et al. (2000) parameterization:

$$k = \sqrt{(600.0/Sc_{skin}) * (0.222\,U_{10}^2 + 0.333\,U_{10})}. \quad (5)$$

The parameterization was based on multiple trace experiment conducted in the southern North Sea during one month in 1992 and 1993 and based on data from March and October 1989.

3. Results and discussion

The global monthly air–sea CO_2 flux variability, the partial pressure of CO_2 in seawater (pCO_{2W}), and gas transfer velocity rates (k) were estimated using FluxEngine software. Values were extracted from these for the two study regions – the GS and BS in the AO (north of 66°) (Fig. 2). The periods from October to April were defined as wintertime and from May to September as summertime. Since wind velocity was used to estimate k, Fig. 1 shows a wide range of empirical formulas. The N2000 quadratic dependence of k on wind speed, which fit the best to AO air–sea interaction measurements (Wrobel and Piskozub, 2016), was chosen for this study. In the AO where the average wind speed during the study period was approximately 8 ± 0.7 m s^{-1} (see Table 1), the average gas transfer velocity rate was 13.0 ± 1.9 cm h^{-1} (Fig. 1). For better proof of results, a statistical summary of the data was calculated (Table 1). The area, as a whole, is a sink of CO_2 with an annual average wind speed of approximately 8 ± 0.7 m s^{-1}, an annual average k of 13.0 ± 1.9 cm h^{-1}, and a concentration of pCO_{2W} (332.4 ± 11.8 μatm) lower than the annual partial pressure of CO_2 in the atmosphere for the year 2010 (382 ± 0.6 μatm). The SST was approximately 3.0 ± 1.6°C and salinity was 34.3.

Table 2 shows the mean monthly variability of the estimated variables. Despite the AO acting as a sink for atmospheric CO_2, considerable variability in ΔpCO_2 was observed

Table 1 Statistics of data used for calculations. Descriptions in rows: k – gas transfer coefficient, U_{10} – 10-m wind speed, pCO_{2W} and pCO_{2A} – seawater and atmospheric partial pressure of CO_2, respectively, ΔpCO_2 – difference in partial pressure, SST – sea surface temperature.

	N	Ave.	Min	Max	St. error	Var.	St. dev
F [mgC m^{-2} day^{-1}]	576	−8.0	−15.4	−4.2	0.1	2.6	1.6
k [cm h^{-1}]	576	13.0	7.9	17.9	0.1	3.5	1.9
U_{10} [m s^{-1}]	576	8.3	5.8	9.7	0.0	0.4	0.7
pCO_{2W} [μatm]	576	332.4	292.7	354.6	0.5	139.2	11.8
ΔpCO_2 [μatm]	576	−50.1	−91.1	−27.7	0.5	152.2	12.3
pCO_{2A} [μatm]	576	382.5	381.2	384.1	0.0	0.4	0.6
SST [°C]	576	3.0		6.5	0.1	2.7	1.6

in space and time (Fig. 6 and Table 2). The pCO_{2W} varies considerably, both spatially and temporarily, as has been shown in recent studies, e.g., Olsen et al. (2003), Omar et al. (2003), Nakaoko et al. (2006), Takahashi et al. (2009), and Sejr et al. (2011). The mean values of partial CO_2 pressure in the air range from 372.5 ± 0.6 μatm in August to 389.1 ± 0.6 μatm in May, while values of partial CO_2 pressure in seawater varied from 309.1 ± 11.8 μatm in August to 348.2 ± 11.8 μatm in February. Bates and Mathis (2009) showed that when SST rises by 1°C pCO_{2W} should increase by up to 8 to 12 μatm/°C. Nakaoko et al. (2006) reported that monthly pCO_{2W} values increased proportionately to increasing SST (in 1994–2001), except in May and June. In June, when SST was above 2°C, pCO_{2W} was higher than 250 μatm, while lower pCO_{2W} was observed when SST was about 1°C. The results from FluxEngine show that when SST increased above 2.5°C, pCO_{2W} was lower than 340 μatm, and when SST decreased below 2.5°C, pCO_{2W} was higher than 340 μatm, except in May. Calculations from FluxEngine indicate the opposite relationship to that demonstrated in Bates and Mathis (2009). During the study period, gas transfer velocity varied from 19.9 ± 1.9 cm h^{-1} in December, when values of wind speed were higher than 10 m s^{-1}, to 6.6 ± 1.9 cm h^{-1} in July when wind speed was lower than 5 m s^{-1}. The strongest winds in the AO were from October to April at mean values of 9.0 ± 0.7 m s^{-1}, while from May to September the values were 6.0 ± 0.7 m s^{-1}.

Fig. 3 shows the relationships between annual mean pCO_{2W} concentrations and air–sea CO_2 fluxes to the north. Over spatial scales, the air–sea CO_2 flux values were strongly positively linked to the partial pressure of CO_2 in seawater (much less than with k) (see Table 3). Regions from the Arctic Circle to the North Pole were sinks of CO_2, and all surface pCO_2 values were below atmospheric levels (pCO_2 in the atmosphere was 380 μatm in 2010), although the Arctic Circle regions were close to equilibrium. The calculated oceanic CO_2 uptake varied between −6 to −16 mgC m^{-2} day^{-1}, and pCO_{2W} concentrations varied between 360 and 290 μatm to the northward. Variations in pCO_{2W} mainly stemmed from to biological activity, changes in sea surface temperature, and water mass transport, which are clearly indicated in Fig. 3 (Garbe et al., 2014; Nakaoko et al., 2006). The SST of the GS and BS was dominated by the inflow of warm North Atlantic Ocean water.

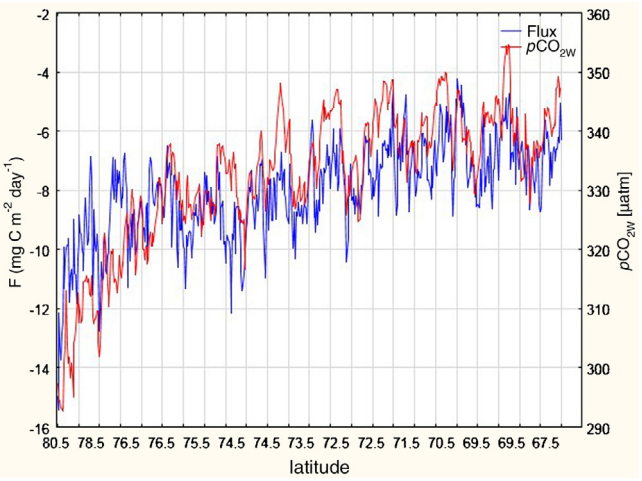

Figure 3 Annual mean pCO_2 in seawater [μatm] and air–sea CO_2 fluxes [mgC m^{-2} day^{-1}].

Fig. 4 illustrates maps of the zonal mean pCO_{2W} in February and August, and Fig. 5 indicates differences between them. In summer, all the pCO_{2W} values in the GS and BS were below atmospheric levels, while in winter pCO_{2W} was close to or higher than atmospheric levels in the BS. These results are in good agreement with those obtained by Cai et al. (2006), Nakaoko et al. (2006) for 1992–2001, and Sejr et al. (2011) for 2006–2009. Calculations from FluxEngine indicate that annual mean values of pCO_{2W} in 2010 were 332.4 ± 11.8 μatm (see Table 1), with mean values in August of 295 ± 11.8 μatm in the GS and 355 ± 11.8 μatm in the BS. Weiss et al. (1992) showed in July 1981 and 1990 that pCO_{2W} concentrations were around 225–230 μatm, while in August 1994–2001 they were around 255 μatm in the GS and 280 μatm in the BS (Nakaoko et al., 2006). During 1995–2003, the annual mean pCO_2 was 313 ± 4.1 μatm in the GS and 292 ± 6.1 μatm in the BS (Arrigo et al., 2010), and in 1995 it was only 282 ± 31 μatm (Takahashi et al., 2002). Generally, the AO is a strong net CO_2 sink; however, there

Table 2 Monthly dynamics of the datasets in the AO. Descriptions in columns: k – gas transfer coefficient, U_{10} – 10-m wind speed, pCO_{2W} and pCO_{2A} – seawater and atmospheric partial pressure of CO_2, respectively, ΔpCO_2 – difference in partial pressure, SST – sea surface temperature.

	F [mgC m^{-2} day^{-1}]	k [cm h^{-1}]	U_{10} [m s^{-1}]	pCO_{2W} [μatm]	ΔpCO_2 [μatm]	pCO_{2A} [μatm]	SST [°C]
Jan	−10.9	18.4	10.6	341.7	−44.2	385.9	2.24
Feb	−8.5	16.6	10	348.2	−39.5	387.8	2.2
Mar	−8.8	16	9.8	346.2	−39.5	385.6	1.92
Apr	−8.4	13.5	8.8	341.5	−44.6	387	1.72
May	−6.9	9.1	7	334.6	−56.5	389.1	2.01
Jun	−4.4	6.8	5.8	328.1	−57.7	384.6	3.44
Jul	−4	6.6	5.2	314.6	−63	377.6	4.99
Aug	−5	7.4	5.9	309.1	−59.4	372.5	4.55
Sep	−6	9.4	6.9	321.3	−52.4	373.11	4.14
Oct	−8.2	16.5	9.4	335.1	−39.1	376.1	3.99
Nov	−11.7	17.5	10	334.2	−48.5	382.7	2.67
Dec	−13.6	19.9	10.9	335	−49	385.2	2.71

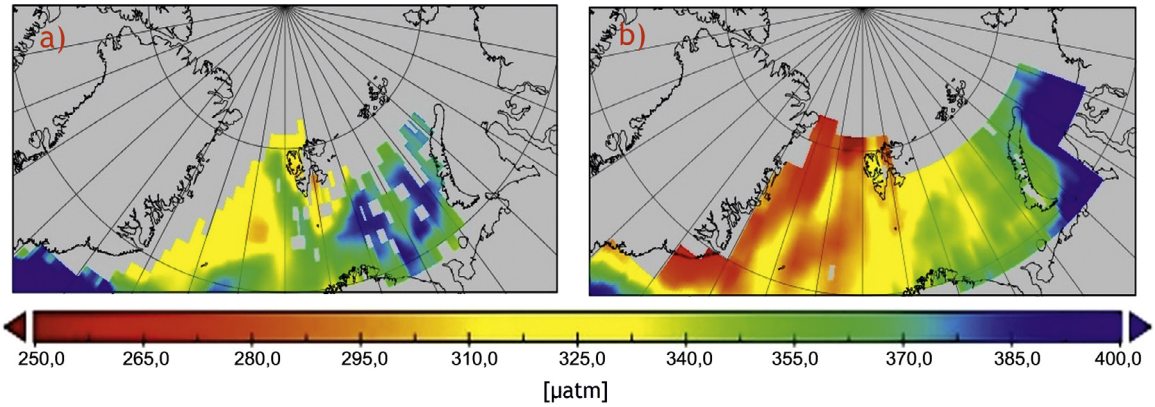

Figure 4 Monthly mean values for pCO_2 in seawater [µatm] in February (a) and August (b).

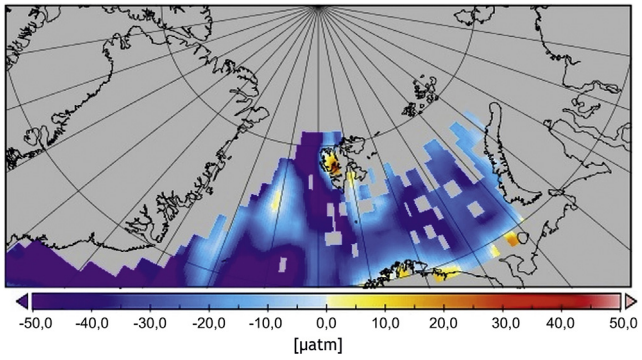

Figure 5 Difference maps for surface water pCO_2 [µatm] values for August–February.

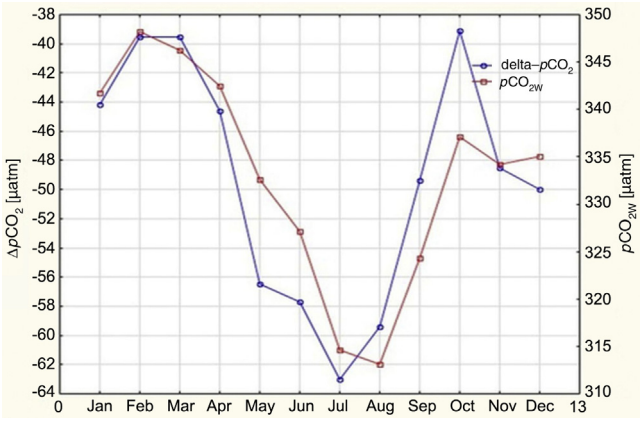

Figure 6 Monthly variability of differences in partial pressure of CO_2 ΔpCO_2 [µatm] and pCO_2 in seawater [µatm].

Table 3 The Pearson linear correlation between datasets in the Arctic Ocean. Descriptions in rows and columns: k – gas transfer coefficient, U_{10} – 10-m wind speed, pCO_{2W} and pCO_{2A} – atmospheric and seawater partial pressure of CO_2, respectively, ΔpCO_2 – difference in partial pressure, SST – sea surface temperature.

	F [mgC m^{-2} day^{-1}]	k [cm h^{-1}]	U_{10} [m s^{-1}]	pCO_{2W} [µatm]	ΔpCO_2 [µatm]	pCO_{2A} [µatm]	SST [°C]
F [mgC m^{-2} day^{-1}]	1.000	0.185	0.042	0.757	0.759	−0.664	0.628
k [cm h^{-1}]	0.185	1.000	0.930	0.636	0.643	−0.663	0.655
U_{10} [m s^{-1}]	0.042	0.930	1.000	0.567	0.570	−0.540	0.457
pCO_{2W} [µatm]	0.757	0.636	0.567	1.000	1.000	−0.833	0.732
ΔpCO_2 [µatm]	0.759	0.643	0.570	1.000	1.000	−0.849	0.745
pCO_{2A} [µatm]	−0.664	−0.663	−0.540	−0.833	−0.849	1.000	−0.878
SST [°C]	0.628	0.655	0.457	0.732	0.745	−0.878	1.000

Table 4 The Pearson linear correlation coefficient between datasets in 2010. Descriptions in columns and rows: k – gas transfer coefficient, U_{10} – 10-m wind speed, pCO_{2W} and pCO_{2A} – seawater and atmospheric partial pressure of CO_2, respectively, ΔpCO_2 – difference in partial pressure, SST – sea surface temperature.

	F [mgC m^{-2} day^{-1}]	k [cm h^{-1}]	U_{10} [m s^{-1}]	pCO_{2W} [µatm]	ΔpCO_2 [µatm]	pCO_{2A} [µatm]	SST [°C]
F [mgC m^{-2} day^{-1}]	1.000	−0.934	−0.928	−0.640	−0.559	−0.475	0.606
k [cm h^{-1}]	−0.934	1.000	0.992	0.761	0.788	0.382	−0.568
U_{10} [m s^{-1}]	−0.928	0.992	1.000	0.826	0.815	0.472	−0.661
pCO_{2W} [µatm]	−0.640	0.761	0.826	1.000	0.877	0.718	−0.858
ΔpCO_2 [µatm]	−0.559	0.788	0.815	0.877	1.000	0.295	−0.562
pCO_{2A} [µatm]	−0.475	0.382	0.472	0.718	0.295	1.000	−0.888
SST [°C]	0.606	−0.568	−0.661	−0.858	−0.562	−0.888	1.000

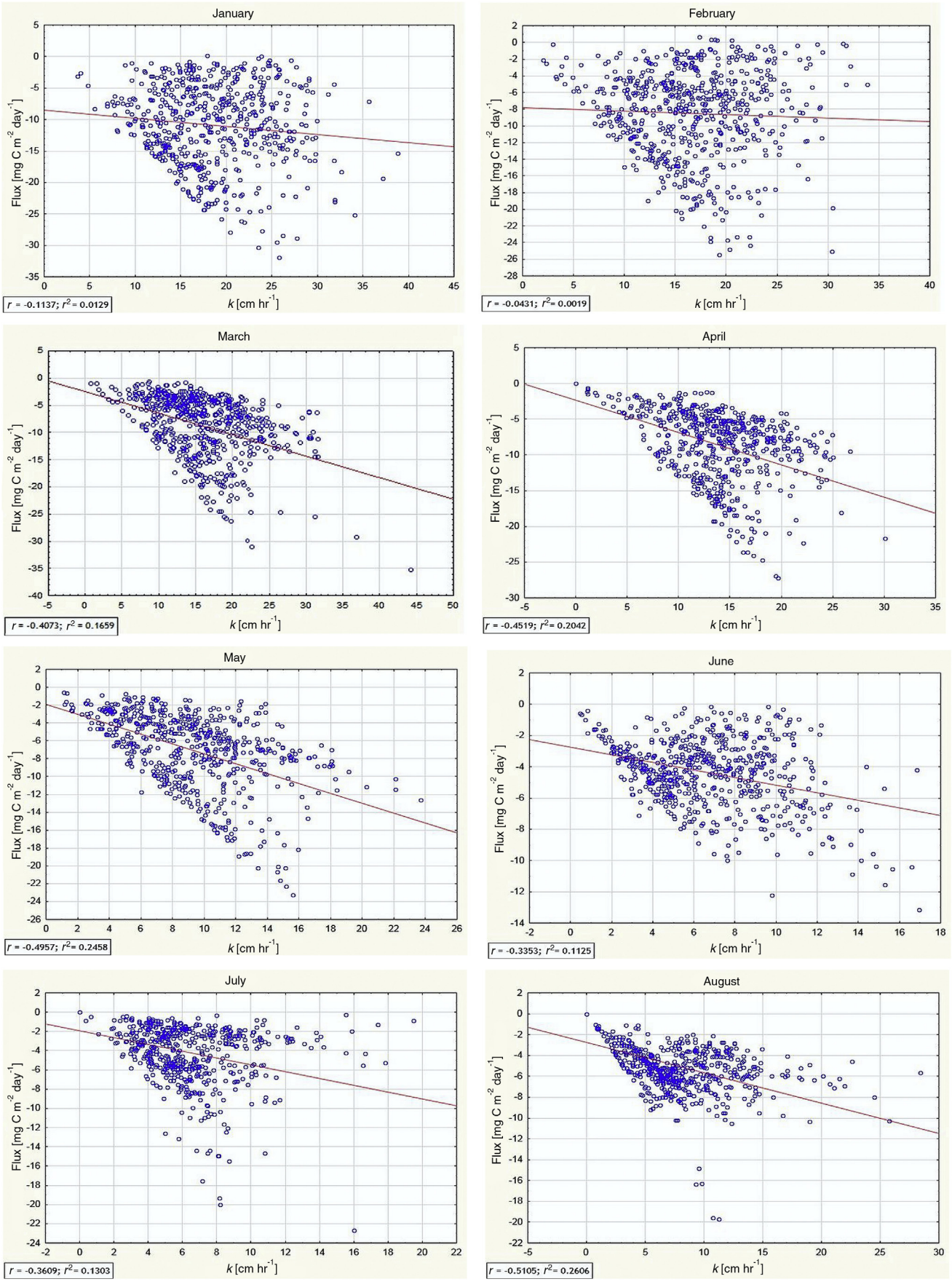

Figure 7 Monthly variations of air—sea CO_2 fluxes [mgC m^{-2} day^{-1}] as a function of gas transfer velocity [cm h^{-1}].

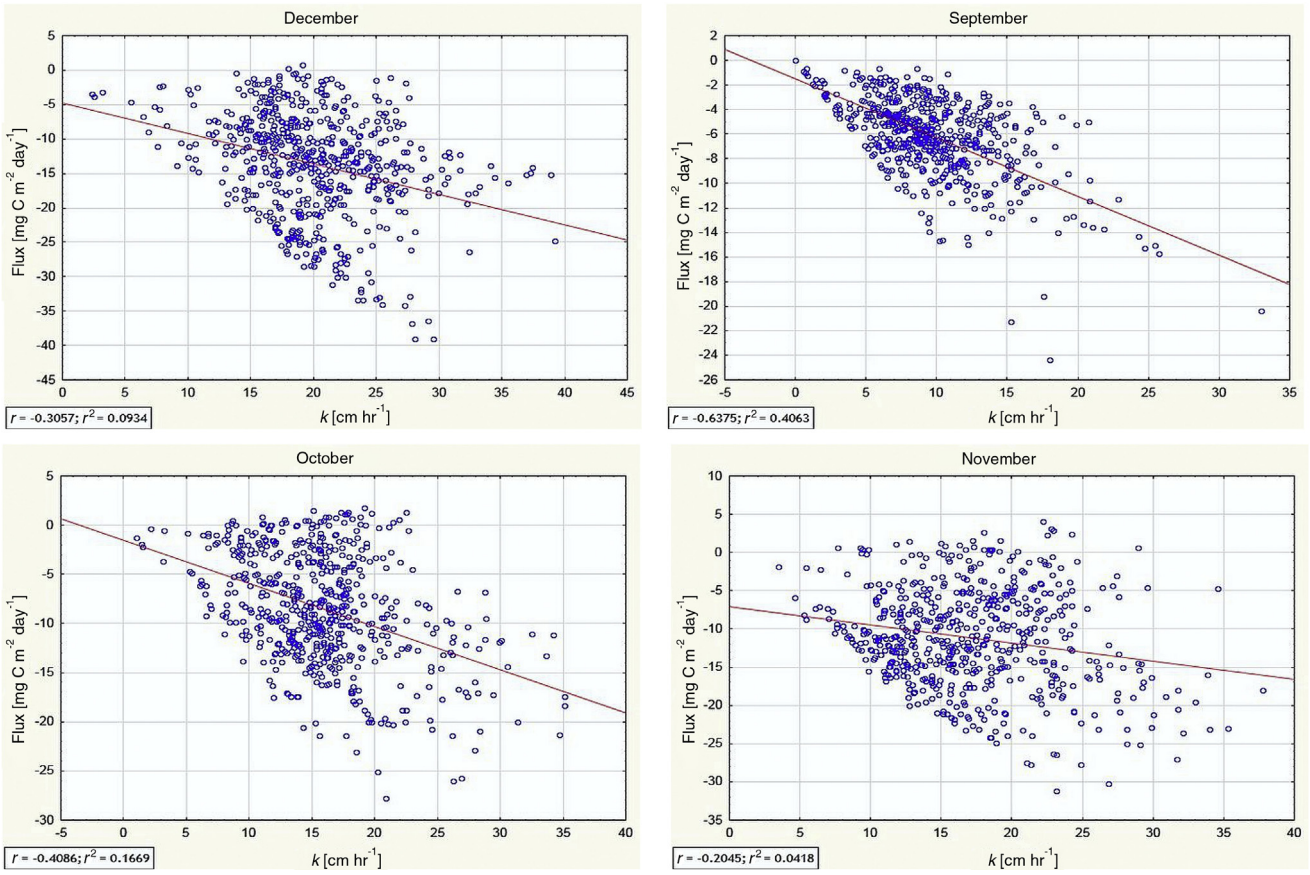

Figure 7. (*Continued*).

are shallow coastal areas where it is a source of CO_2 to the atmosphere, caused by river outputs and sea ice melting (Bates and Mathis, 2009). Seasonal changes in biological activity (phytoplankton primary production, PP), sea water warming and cooling, and the volume of CO_2 exchange caused seasonal changes in surface pCO_2. In wintertime, during the study, when the temperature of sea water was lower than in summer, pCO_{2W} levels were higher in the open water of the GS and BS in February (310—370 and 355—400 μatm, respectively) than in August (250—325 and 325—370 μatm, respectively) (Fig. 4). Additionally, in the GS, in both February and August, the concentration of pCO_{2W} was lower (Fig. 4) with differences in absolute values higher than in the BS (Fig. 5). This observation agrees well with earlier results obtained by Takahashi et al. (2002), Olsen et al. (2003), and Nakaoko et al. (2006). During summertime, surface pCO_{2W} values decreased, in spite of seasonal warming and oceanic CO_2 uptake increased thanks to high CO_2 exchange (Bates and Mathis, 2009). These processes were counterbalanced by the uptake of CO_2 in summertime by phytoplankton that decreased pCO_2.

Fig. 5 shows that inside the Arctic fjord the difference between pCO_2 in the summer and the winter was caused by lower surface-water pCO_2 levels resulting from sea ice melt, dissolution of $CaCO_3$, primary production, and strong stratification of the water column inside the fjord. Melting sea ice in the summer caused low pCO_2 levels, but melt water ponds were also pCO_{2A} sinks (Sejr et al., 2011; Semiletov et al., 2004). The results from estimations contrast with those gathered by Omar et al. (2007) and Sejr et al. (2011), and they show that fjords and nearby lands in the AO are places where physical process do not exceed biological CO_2 uptake because of runoff from lands, but in the open water area of the AO the opposite was found. This could steam from the fjords not being well represented in the data, and it could imply some underestimation of ΔpCO_2 rates. It does indicate, though, that more study of the shallow and marginal areas is required.

Fig. 6 shows the monthly values of pCO_{2W} and ΔpCO_2. Over the temporal scale, of the study period, all surface pCO_2 levels were below atmospheric levels (average 380 μatm) resulting in negative ΔpCO_2. The calculated pCO_{2W} and ΔpCO_2 values show seasonal variation of about 39 and 24 μatm, respectively, with two maxima for pCO_{2W} in February and October and one minima in August, and two minima for ΔpCO_2 in March and October and one maxima in July. These observations agree well with the previous studies (Nakaoko et al., 2006; Takahashi et al., 2009). The ΔpCO_2 values increased (at a rate of 5 μatm) compared to previous results obtained by Takahashi et al. (2009). The seasonal difference in ΔpCO_2 (strong negative values in the summertime) resulted from the biological drawdown of CO_2. Differences in the partial pressure of CO_2 were very strongly correlated with changes in the partial pressure of CO_{2W}, especially in wintertime, when the average water temperature was higher than the air temperature (see also the discussion in Table 2).

Figs. 7 and 8 show regression lines, correlations, and determination coefficients between air—sea CO_2 fluxes,

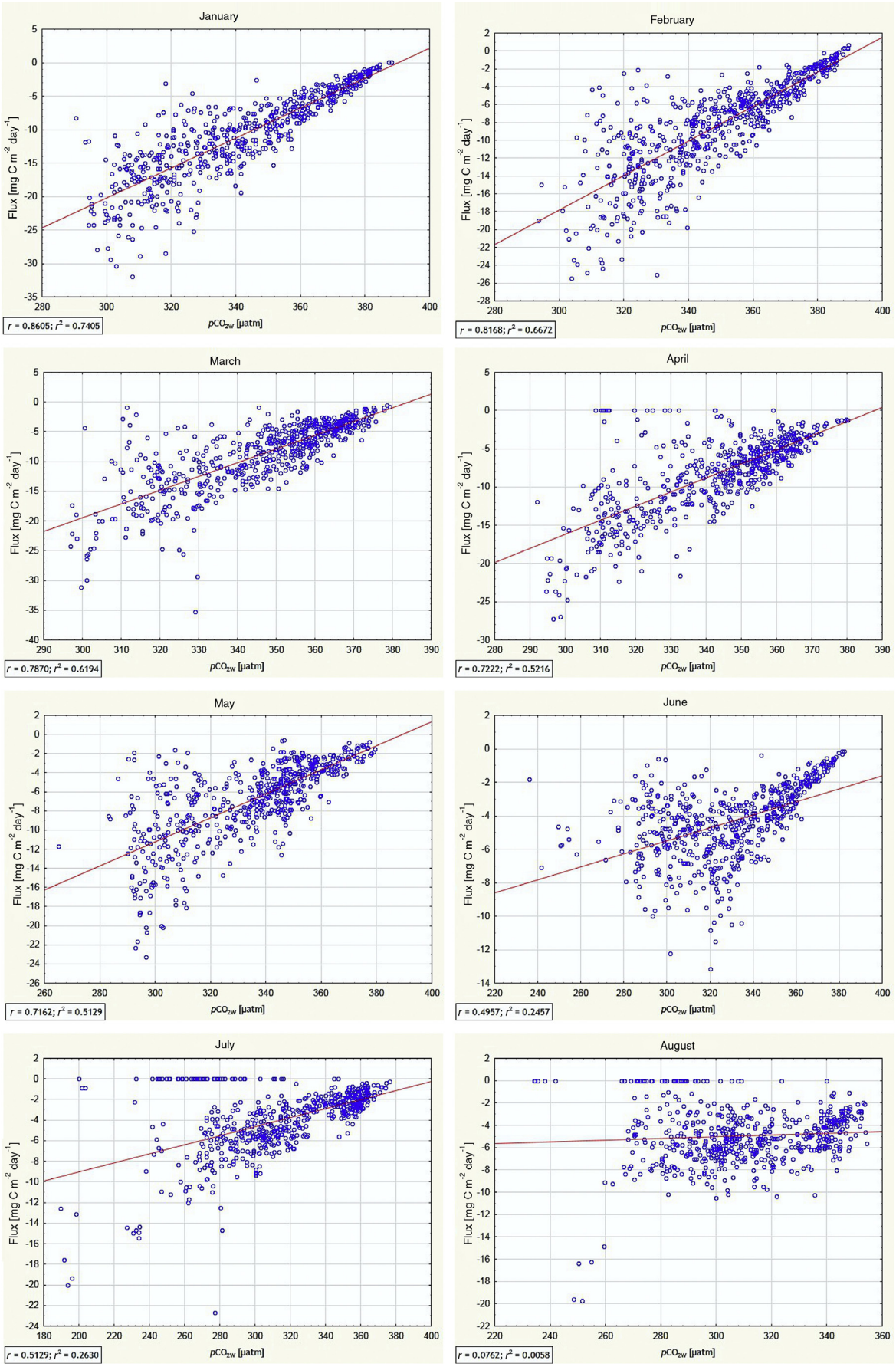

Figure 8 Monthly dynamics of air–sea CO_2 flux [mgC m^{-2} day^{-1}] as a function of pCO_2 in seawater [µatm].

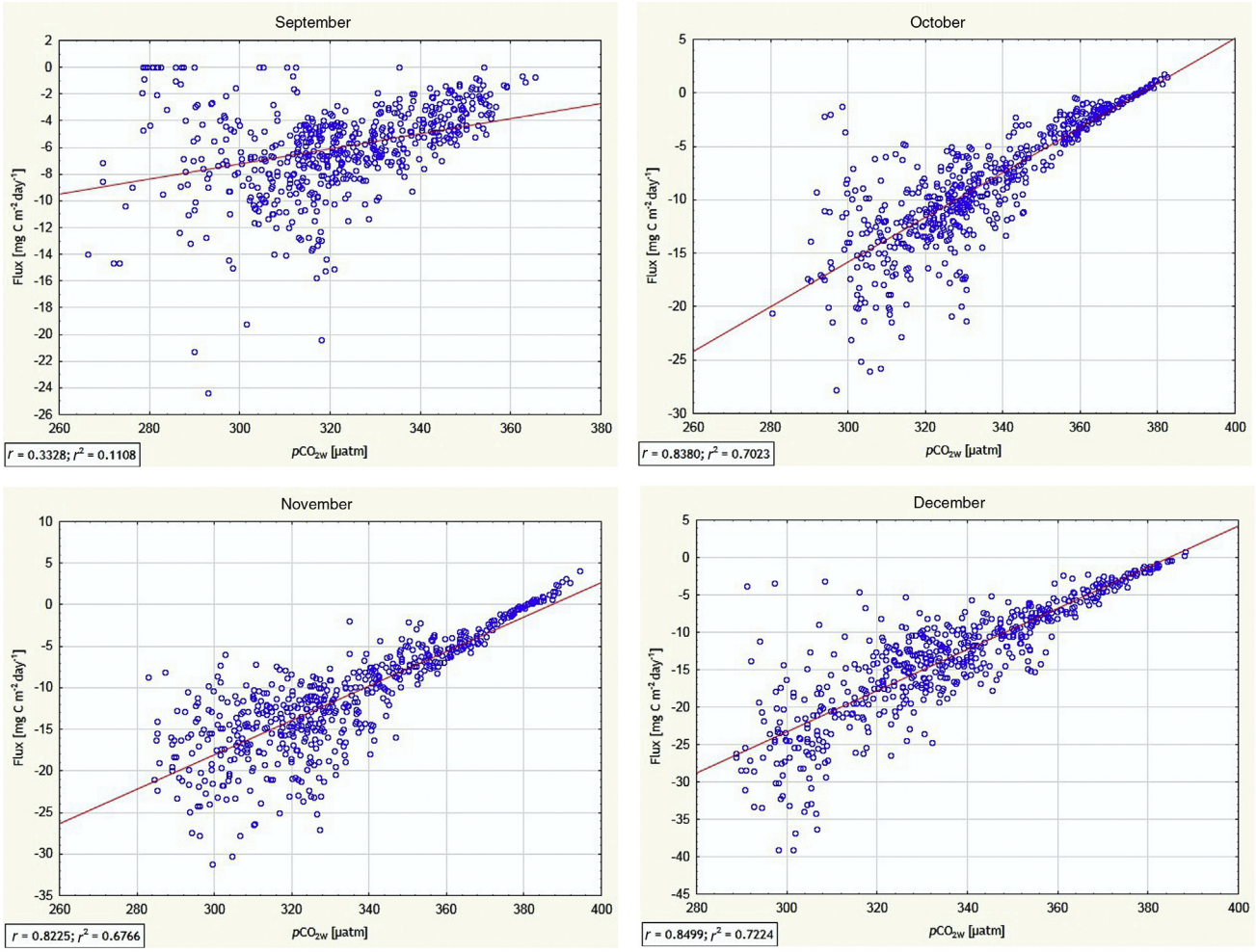

Figure 8. (*Continued*).

pCO_{2W}, and k for individual months. The correlation coefficient (r) represents the linear relationship between two variables and the determination coefficient (r^2) represents the proportion of common variation between the two variables (StatSoft Inc., 2013). Over spatial scales, fluxes were better correlated with pCO_{2W} than with gas transfer velocity during each month. In the relationship between air–sea fluxes and k, in May, August, and September more than 20% of variability in fluxes was explained by k (typically less than 20%; Fig. 7). More than 50% of variability in fluxes was explained by pCO_{2W} (except from June to September, when it was less than 20%; Fig. 8). In summertime, CO_2 flux variability was controlled by k, as a function of sea ice cover. The results reflect those obtained by Doney et al. (2009) and Couldrey et al. (2016). They demonstrated that variability in k contributes to only approximately 35% of the global interannual flux variability, while ΔpCO_2 contributes 60% of total variability.

Fig. 9 shows spatiotemporal mean air–sea CO_2 fluxes in the GS and BS during study period using the Nightingale et al. (2000) k parameterization. Cai et al. (2006) estimated that the continental shelves of the AO were responsible for the total uptake of atmospheric CO_2 of 52 TgC a^{-1}, equivalent to an average air–sea CO_2 flux of −12 gC m^{-2} a^{-1}. The total uptake for the BS was estimated to be about 3.2 TgC a^{-1} or a flux of −4.38 gC m^{-2} a^{-1}. Following the methods described in Table S1 in Cai et al. (2006), the total uptake of atmospheric CO_2 on the continental shelves of the GS and BS was estimated as 3.6 TgC a^{-1} and the average air–sea CO_2 fluxes were estimated about −3.62 gC m^{-2} a^{-1}. As can be seen, the GS was a stronger net sink of CO_2 in winter (approximately −12 mgC m^{-2} day^{-1}), while the BS was a very weak sink for CO_2 that was close to equilibrium. There were seasonal changes throughout the year. The annual mean air–sea CO_2 flux for the whole study area was −8.0 mgC m^{-22} day^{-1} (see Table 1). This is because the BS had higher SST than the GS because of the inflow of warm water via the North Atlantic Current (Land et al., 2013). Additionally, as is shown in Fig. 3, air–sea CO_2 fluxes are strongly positively correlated with pCO_{2W} over spatial scales. Estimates for the central GS are similar to previous results: 52 gC m^{-2} a^{-1} for the 1992–2001 period (Nakaoko et al., 2006), 25 gC m^{-2} a^{-1} for 2006, and 42 gC m^{-2} a^{-1} for 2009 (Sejr et al., 2011). Most areas of the BS became CO_2 sources in summer and fall, which is likely to be from the effect of sea–water temperature changes. During spring, no upward CO_2 flux was observed in the Arctic sector of the Atlantic Ocean. The air–sea CO_2 flux from the atmosphere decreased slightly

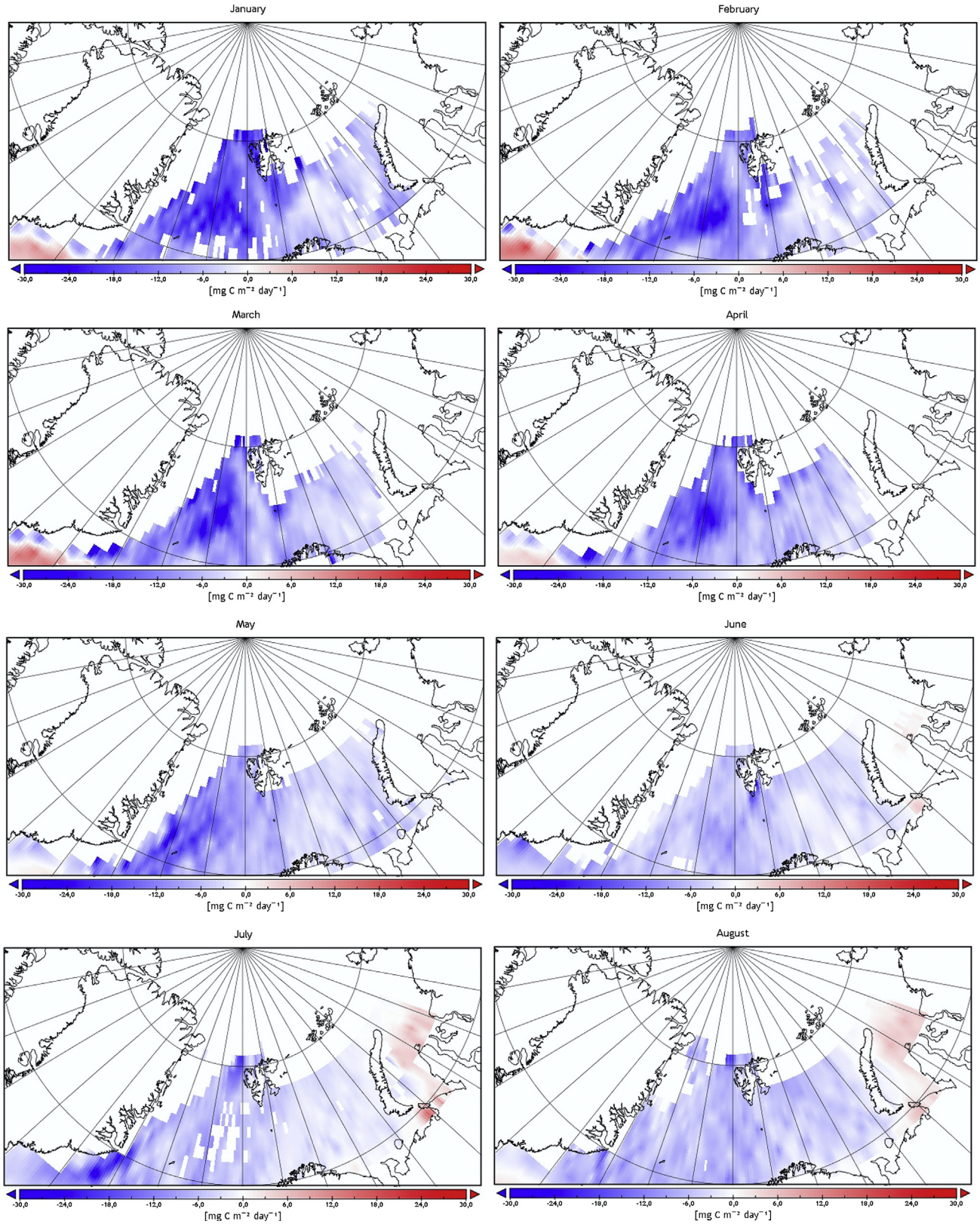

Figure 9 Monthly mean values for air–sea CO_2 fluxes [mgC m^{-2} day^{-1}] combined using *k* parameterization by Nightingale et al. (2000). Blue is absorbing, red is emitting. (For interpretation of the references to color in this figure legend, the reader is referred to the web version of the article.)

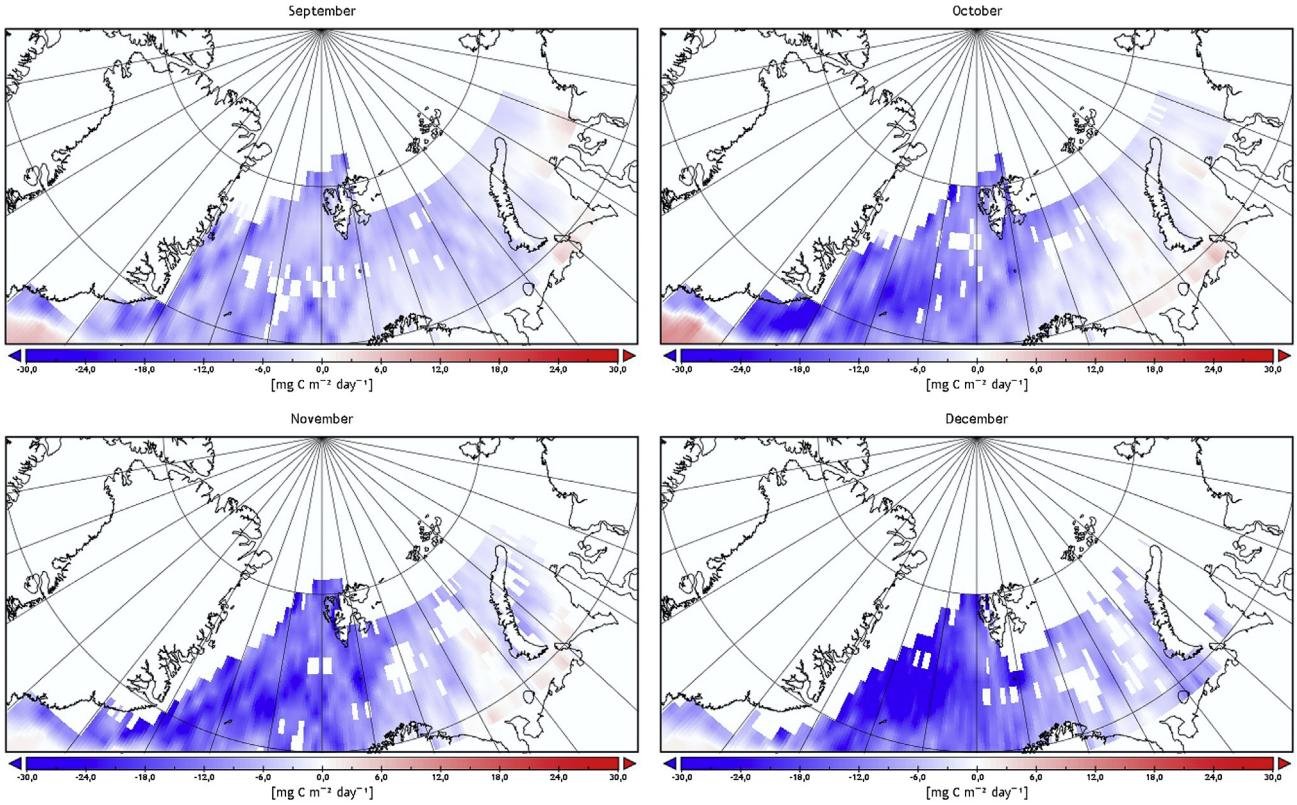

Figure 9. (*Continued*).

during June and July (Fig. 9), which was because of a steep decrease in average wind speed and low pCO_2; these values were in good agreement with results reported by Arrigo et al. (2010).

The relationships among the variables influencing gas fluxes on spatial and temporal scales are shown in Tables 3 and 4. In general, there were very few positive correlations between air–sea CO_2 fluxes and k over spatial scales ($r = 0.185$, $p < 0.05$), and very strong negative correlations over temporal scales ($r = -0.935$, $p < 0.05$) with moderate negative correlations in individual months (Fig. 7). In wintertime, when the wind was stronger (hence higher k), than in summertime, the rates of air–sea CO_2 fluxes were up to -10 mgC m^{-2} day^{-1}. In June and July, the rates of air–sea CO_2 exchange were small (<5 mgC m^{-2} day^{-1}) when compared to the annual average (Table 1). These results match those derived by Nakaoko et al. (2006) for the GS and BS. In summertime, the majority of measurements were much less scattered around the trend line than in wintertime when the values were more scattered (Fig. 7). The fluxes across the air–sea interface were controlled by SST, wave breaking, friction velocity, sea state, turbulence, etc. (Goddijn-Murphy et al., 2016; Nightingale et al., 2000). The rate of transfer across the sea surface is usually a parameter that is a function of wind speed at 10 m. a.s.l. However, there were also other factors that influence air–sea CO_2 fluxes, such as surface films, fetch, and chemical enhancement (McGillis et al., 2001; Wanninkhof et al., 2009). Strong positive correlations between pCO_2 and air–sea fluxes ($r = 0.757$, $p < 0.05$) over spatial scales and quite strong negative correlations over temporal scales ($r = -0.640$, $p < 0.05$) were noted (Fig. 8). In the AO, the spatial variability in pCO_{2W} showed quite strong positive correlations with SST ($r = 0.732$, $p > 0.05$), while temporal variability showed even stronger negative correlations with SST ($r = -0.858$, $p > 0.05$; Tables 3 and 4).

4. Conclusions

This study examined the effect of monthly changes in gas transfer velocity and ΔpCO_2 in controlling air–sea CO_2 fluxes in the Greenland Sea and the Barents Sea, during a one year period. It also examined the following testable hypothesis: air–sea CO_2 fluxes over one year are dependent on both ΔpCO_2 and k. Results from FluxEngine showed that air–sea CO_2 fluxes had fewer positive correlations with gas transfer velocity (k) over spatial scales (Table 3), and almost perfect negative correlations over temporal scales (Table 4) with moderate negative correlations within individual months (Fig. 7). Additionally, there were strong positive correlations between pCO_2 and air–sea fluxes over spatial scales (Table 3) and quite strong negative correlations over temporal scales (Table 4), with strong positive correlations within individual months (Fig. 8). In the relationships between air–sea fluxes and gas transfer velocity in May, August, and September, more than 20% of the variability in fluxes was explained by k (typically it was less than 20%; Fig. 7). More than 50% of variability in fluxes was explained by pCO_{2W} (except from June to September, where it was less than 20%; Fig. 8). The results indicate that the variability in wind speed, and, hence, gas transfer velocity, plays a major role over temporal

scales, while ΔpCO_2, and hence pCO_{2w}, plays a major role over spatial scales in determining the monthly variation of CO_2 uptake in this area. On these timescales it is critical to obtain estimates of pCO_2 and k for accurate flux variability to be derived. We can predict the future state of the global carbon cycle only if we improve understanding the carbon cycle mechanisms of this area by using our ability to diagnose past change and analyze present variability.

As can be seen, even using satellite data is insufficient for specifying the mechanisms controlling carbon uptake in the Arctic Ocean. There are many gaps in the data from this region, and many uncertainties in approaches to estimating air—sea fluxes. We still do not know exactly how sea ice melting influences carbon uptake or how each component of the biological and physical carbon dioxide pumps influence air—sea flux values. Two relatively simple improvements may prevent the data gaps in projecting and evaluating carbon fluxes in this region in the future — a use of new techniques for interpolating data as well as a use of commercial ships for transporting and deploying sampling equipment in the winter.

Acknowledgements

The publication was financed with funds from Leading National Research Centre (KNOW) received by the Centre for Polar Studies for the period 2014—2018; OceanFlux Greenhouse Gases Evolution, a project funded by the European Space Agency, ESRIN Contract No. 4000112091/14/I-LG; and GAME project of National Science Centre No. DEC-2012/04/A/NZ8/00661. I would also like to thank Jacek Piskozub for significant corrections and comments.

References

Arrigo, K.R., van Dijken, G.L., Pabi, S., 2008. Impact of a shrinking Arctic ice cover on marine primary production. Geophys. Res. Lett. 35 (19), L19603, 6 pp., http://dx.doi.org/10.1029/2008GL035028.

Arrigo, K.R., Pabi, S., van Dijken, G.L., Maslowski, W., 2010. Air—sea flux of CO_2 in the Arctic Ocean, 1998—2003. J. Geophys. Res. Biogeosci. 115 (G4), 15 pp., http://dx.doi.org/10.1029/2009JG001224.

Ashton, I.G., Shutler, J.D., Land, P.E., Woolf, D.K., Quartly, G.D., 2016. A sensitivity analysis of the impact of rain on regional and global sea—air fluxes of CO_2. PLOS ONE 11 (9), e0161105, 18 pp., http://dx.doi.org/10.1371/journal.pone.0161105.

Bates, N.R., 2012. Multi-decadal uptake of carbon dioxide into subtropical mode water of the North Atlantic Ocean. Biogeoscience 9 (7), 2649—2659, http://dx.doi.org/10.5194/bg-9-2649-2012.

Bates, N.R., Mathis, J.T., 2009. The Arctic Ocean marine carbon cycle: evaluation of air—sea CO_2 exchanges, ocean acidification impacts and potential feedbacks. Biogeosciences 6 (11), 2433—2459, http://dx.doi.org/10.5194/bg-6-2433-2009.

Boutin, J., Etcheto, J., Merlivat, L., Rangama, Y., 2002. Influence of gas exchange coefficient parameterization on seasonal and regional variability of CO_2 air—sea fluxes. Geophys. Res. Lett. 29 (8), 23-1—23-4, http://dx.doi.org/10.1029/2001GL013872.

Cai, W.-J., Dai, M., Wang, Y., 2006. Air—sea exchange of carbon dioxide in ocean margins: a province-based synthesis. Geophys. Res. Lett. 33 (12), L12603, http://dx.doi.org/10.1029/2006GL026219.

Couldrey, M.P., Oliver, K.I.C., Yool, A., Halloran, P.R., 2016. On which timescales do gas transfer velocities control North Atlantic CO_2 flux variability? Global Biogeochem. Cycl. 30 (5), 787—802, http://dx.doi.org/10.1002/2015GB005267.

Dai, A., Qian, T., Trenberth, K.E., Millimian, J.D., 2009. Changes in continental freshwater discharge from 1948 to 2004. J. Climate 22 (10), 2773—2792, http://dx.doi.org/10.1175/2008JCLI2592.1.

Doney, S.C., Lima, I., Feely, R.A., Glover, D.M., Lindsey, K., Mahowald, N., Moore, J.K., Wanninkhof, R., 2009. Mechanisms governing interannual variability in upper-ocean inorganic carbo system and air—sea CO_2 fluxes: physical climate and atmospheric dust. Deep-Sea Res. Pt. II 56 (8—10), 640—655, http://dx.doi.org/10.1016/j.dsr2.2008.12.006.

Else, B.G.T., Papakyriakou, T.N., Galley, R.J., Drennan, W.M., Miller, L.A., Thomas, H., 2011. Wintertime CO_2 fluxes in an Arctic polynya using eddy covariance: evidence for enhanced air—sea gas transfer during ice formation. J. Geophys. Res. 116 (C9), C00G03, 15 pp., http://dx.doi.org/10.1029/2010JC006760.

Garbe, C.S., Rutgersson, A., Boutin, J., de Leeuw, G., Delille, B., Fairall, C.W., Gruber, N., Hare, J., Ho, D.T., Johnson, M.T., Nightingale, P.D., Pettersson, H., Piskozub, J., Sahlee, E., Tsai, W., Ward, B., Woolf, D.K., Zappa, C.J., 2014. Transfer across the air—sea interface. In: Liss, P.S., Johnson, M.T. (Eds.), Ocean—Atmosphere Interactions of Gases and Particles. Springer-Earth Sys. Sciences, Berlin, Heidelberg, 55—111.

Goddijn-Murphy, L., Woolf, D.K., Land, P.E., Shutler, J.D., Donlon, C., 2015. The OceanFlux Greenhouse Gases methodology for deriving a sea surface climatology of CO_2 fugacity in support of air—sea gas flux studies. Ocean Sci. 11 (4), 519—541, http://dx.doi.org/10.5194/os-11-519-2015.

Goddijn-Murphy, L., Woolf, D.K., Callaghan, A.H., Nightingale, P.D., Shutler, J.D., 2016. A reconciliation of empirical and mechanistic models of the air—sea gas transfer velocity. J. Geophys. Res. 121 (1), 818—835, http://dx.doi.org/10.1002/2015JC011096.

Gruber, N., 2009. Carbon cycle: fickle trends in the ocean. Nature 458 (7235), 155—156, http://dx.doi.org/10.1038/458155a.

Gruber, N., Keeling, C.D., Bates, N.P., 2003. Interannual variability in the North Atlantic Ocean carbon sink. Science 298 (5602), 2374—2378, http://dx.doi.org/10.1126/science.1077077.

Gurgul, H., 2002. Białe Pustynie — Arktyka. Wyd. Kurpisz. Poznań, 4—30.

Ho, D.T., Law, C.S., Smith, M.J., Schlosser, P., Harvey, M., Hill, P., 2006. Measurements of air—sea gas exchange at high wind speeds in the Southern Ocean: implications for global parameterizations. Geophys. Res. Lett. 33 (16), L16611, http://dx.doi.org/10.1029/2006GL026817.

IPCC, 2013. Carbon and other biogeochemical cycles. In: Stocker, T.F., Qun, D., Plattner, G.-K., Tignor, W., Allen, S.K., Boschung, J., Nauels, A., Xia, Y., Bex, V., Midgley, P.M. (Eds.), Climate Change 2013: The Physical Science Basis. Contribution of Working Group I to the Fifth Assessment Report of the Intergovernmental Panel on Climate Change. Cambridge Univ. Press, Cambridge, 470—516.

Kondo, F., Tsukamoto, O., 2012. Comparative CO_2 flux measurements by eddy covariance technique using open- and closed-path gas analysers over the Equatorial Pacific Ocean. Tellus B 64 (17511), 1—12, http://dx.doi.org/10.3402/tellusb.v64i0.17511.

Kulinski, K., She, J., Pempkowiak, J., 2011. Short and medium term dynamics of the carbon exchange between the Baltic Sea and the North Sea. Cont. Shelf Res. 31 (15), 1611—1619, http://dx.doi.org/10.1016/j.csr.2011.07.001.

Land, P.E., Shutler, J.D., Cowling, R.D., Woolf, D.K., Walker, P., Findlay, H.S., Upstill-Goddard, R.C., Donlon, C.J., 2013. Climate change impacts on sea—air fluxes of CO_2 in three Arctic seas: a sensitivity study using Earth observation. Biogeosciences 10 (12), 8109—8128, http://dx.doi.org/10.5194/bg-10-8109-2013.

Landschützer, P., Gruber, N., Bakker, D.C.E., Schuster, U., 2014. Recent variability of the global ocean carbon sink. Global

Biogeochem. Cycl. 28 (9), 927–949, http://dx.doi.org/10.1002/2014GB004853.

Le Quéré, C., Andres, R.J., Boden, T., Conway, T., Houghton, R.A., House, J.I., Marland, G., Peters, G.P., van der Werf, G.R., Ahlström, A., Andrew, R.M., Bopp, L., Canadell, J.G., Ciais, P., Doney, S.C., Enright, C., Friedlingstein, P., Huntingford, C., Jain, A.K., Jourdain, C., Kato, E., Keeling, R.F., Klein Goldewijk, K., Levis, S., Levy, P., Lomas, M., Poulter, B., Raupach, M.R., Schwinger, J., Sitch, S., Stocker, B.D., Viovy, N., Zaehle, S., Zeng, N., 2013. The global carbon budget 1959–2011. Earth Syst. Sci. Data 5, 165–185, http://dx.doi.org/10.5194/essd-5-165-2013.

Le Quéré, C., Andrew, R.M., Canadell, J.G., Sitch, S., Korsbakken, J.I., Peters, G.P., Manning, A.C., Boden, T.A., Tans, P.P., Houghton, R.A., Kelling, R.F., Alin, S., Andrews, O.D., Anthoni, P., Barbero, L., Bopp, L., Chevallier, F., Chini, L.P., Ciais, P., Currie, K., Delire, C., Doney, S.C., Friedlingstein, P., Gkritzalis, T., Harris, I., Hauck, J., Haverd, V., Hoppema, M., Goldewijk, K. K., Jain, A.K., Kato, E., Körtzinger, A., Landschützer, P., Lefèvre, N., Lenton, A., Lienert, S., Lombardozzi, D., Melton, J.R., Metzl, N., Millero, F., Monteiro, P.M.S., Munro, D.R., Nabel, J.E.M.S., Nakaoko, S.I., O'Brien, K., Olsen, A., Omar, A.M., Ono, T., Pierrot, D., Poulter, B., Rödenbeck, C., Salisbury, J., Schuster, U., Schwinger, J., Séférian, R., Skjelvan, I., Stocker, B.D., Sutton, A.J., Takahashi, T., Hanqin, T., Tilbrook, B., van der Laan-Luijkx, I.T., van der Werf, G.R., Viovy, N., Walker, A.P., Wiltshire, A.J., Zaehle, S., 2016. Global Carbon budget 2016. Earth Syst. Sci. Data 8 (2), 605–649, http://dx.doi.org/10.5194/essd-8-605-2016.

Le Quéré, C., Orr, J.C., Monfray, P., Aumont, O., Madec, G., 2000. Interannual variability of the oceanic sink of CO_2 from 1979 through 1997. Global Biogeochem. Cycl. 14 (4), 1247–1265, http://dx.doi.org/10.1029/1999GB900049.

Le Quéré, C., Takahashi, T., Buitenhuis, E.T., Rödenbeck, C., Sutherland, S.C., 2010. Impact of climate change and variability on the global oceanic sink of CO_2. Global Biogeochem. Cycl. 24 (4), GB4007, http://dx.doi.org/10.1029/2009GB003599.

Lefèvre, N., Watson, A.J., Olsen, A., Rios, A.F., Perez, F.F., Johannessen, T., 2004. A decrease in the sink for atmospheric CO_2 in the North Atlantic. Geophys. Res. Lett. 31 (7), L07306, http://dx.doi.org/10.1029/2003GL018957.

Lefèvre, N., Watson, A.J., Watson, A.R., 2005. A comparison of multiple regression an neutral network techniques for mapping in situ pCO_2 data. Tellus B 57 (5), 375–384, http://dx.doi.org/10.1111/j.1600-0889.2005.00164.x.

MacGilchrist, G.A., Naveira Garabato, A.C., Tsubouchi, T., Bacon, S., Torres-Valdés, S., Azetsu-Scott, K., 2014. The Arctic Ocean carbon sink. Deep-Sea Res. Pt. I 86, 39–55, http://dx.doi.org/10.1016/j.dsr.2014.01.002.

McGillis, W.R., Edson, J.B., Hare, J.E., Fairall, C.W., 2001. Direct covariance air–sea CO_2 fluxes. J. Geophys. Res. 106 (C8), 16729–16745, http://dx.doi.org/10.1029/2000JC000506.

Merchant, C.J., Embury, O., Rayner, N.A., Berry, D.I., Corlett, G.K., Lean, K., Veal, K.L., Kent, E.C., Llewellyn-Jones, D.T., Remedios, J.J., Saunders, R., 2012. A 20 year independent record of sea surface temperature for climate from Along-Track Scanning Radiometers. J. Geophys. Res. 117 (C12), C12013, 18 pp., http://dx.doi.org/10.1029/2012JC008400

Minnett, P., Kaiser-Weiss, A., 2012. Discussion Document: Near-surface Oceanic Temperature Gradients, https://www.ghrsst.org/wp-content/uploads/2016/10/SSTDefinitionsDiscussion.pdf.

Nakaoko, S.I., Aoki, A., Nakazawa, T., Hashida, G., Morimoto, S., Yamanouchi, T., Yoshikawa-Inoue, H., 2006. Temporal and spatial variations of oceanic pCO_2 and air–sea CO_2 flux in Greenland Sea and Barents Sea. Tellus B 58 (2), 148–616, http://dx.doi.org/10.1111/j.1600-0889.2006.00178.

Nightingale, P.D., Malin, G., Law, C.S., Watson, A.J., Liss, P.S., Liddicoat, M.I., Boutin, J., Upstill-Goddard, R.C., 2000. In situ evaluation of air–sea gas exchange parameterizations using novel conservative and volatile tracers. Global Biogeochem. Cycl. 14 (1), 373–387, http://dx.doi.org/10.1029/1999GB900091.

Olsen, A., Bellerby, R.G.J., Johannessen, T., Omar, A.M., Skjelvan, I., 2003. Interannual variability in the wintertime air–sea flux of carbon dioxide in the northern North Atlantic 1981–2001. Deep-Sea Res. Pt. I 50 (11), 1323–1338, http://dx.doi.org/10.1016/S0967-0637(03)00144-4.

Omar, A.M., Johannessen, T., Kaltin, S., Olsen, A., 2003. Anthropogenic increase of oceanic pCO_2 in the Barents Sea surface water. J. Geophys. Res. 108 (C12), 18-1–18-8, http://dx.doi.org/10.1029/2002JC001628.

Omar, A.M., Johannessen, T., Olsen, A., Kaltin, S., Rey, F., 2007. Seasonal and interannual variability of the air–sea CO_2 flux in the Atlantic sector of the Barents Sea. Mar. Chem. 104 (3), 203–213, http://dx.doi.org/10.1016/j.marchem.2006.11.002.

Piechura, J., Walczowski, W., 2009. Warming of the West Spitsbergen Current and sea ice north of Svalbard. Oceanologia 51 (2), 147–164, http://dx.doi.org/10.5697/oc.51-2.147.

Polyakov, I.V., Alekseev, G.V., Timokhov, L.A., Bhatt, U.S., Colony, R. L., Simmons, H.L., Walsh, D., Walsh, J.E., Zakharov, V.F., 2004. Variability of the Intermediate Atlantic Water of the Arctic Ocean over the last 100 years. J. Climate 17 (23), 4485–4497, http://dx.doi.org/10.1175/JCLI-3224.1.

Repina, I.A., Semiletov, I.P., Smirnov, A.S., 2007. Eddy correlation measurements of air–sea CO_2 fluxes in the Laptev Sea in the summer period. Doklady Earth Sci. 413 (2), 452–456, http://dx.doi.org/10.1134/S1028334X07030300.

Rödenbeck, C., 2005. Estimating CO_2 Sources and Sinks From Atmospheric Mixing Ratio Measurements Using a Global Inversion of Atmospheric Transport. Max-Planck Institute for Biogeochemistry, Jena, 53 pp.

Sabine, C.L., Feely, R.A., Gruber, N., Key, R.M., Lee, K., Bullister, J. L., Wanninkhof, R., Wong, C.S., Wallace, D.W.R., Tilbrook, B., Millero, F.J., Peng, T.-H., Kozyr, A., Ono, T., Ríos, A.F., 2004. The oceanic sink for anthropogenic CO_2. Science 305 (5682), 367–371, http://dx.doi.org/10.1126/science.1097403.

Schuster, U., McKinley, G.A., Bates, N., Chevallier, F., Doney, S.C., Fay, A.R., González-Dávila, M., Gruber, N., Jones, S., Krijnen, J., Landschützer, P., Lefèvre, N., Manizza, M., Mathis, J., Metzl, N., Olsen, A., Ríos, A.F., Rödenbeck, C., Santana-Casiano, J.M., Takahashi, T., Wanninkhof, R., Watson, A.J., 2013. An assessment of the Atlantic and Arctic sea–air CO_2 fluxes, 1990–2009. Biogeosciences 10 (1), 607–627, http://dx.doi.org/10.5194/bg-10-607-2013.

Sejr, M.K., Krause-Jensen, D., Rysgaard, R., Sørensen, L.L., Christensen, P.B., Glud, R.N., 2011. Air–sea flux of CO_2 in arctic coastal waters influenced by glacial melt water and sea ice. Tellus B 63 (5), 815–822.

Semiletov, I.P., Makshtas, A., Akasofu, S.-I., Andreas, L.A., 2004. Atmospheric CO_2 balance: the role of the Arctic sea ice. Geophys. Res. Lett. 31 (5), L05121, 4 pp., http://dx.doi.org/10.1029/2003GL017996.

Shutler, J.D., Piolle, J.-F., Land, P.E., Woolf, D.K., Goddijn-Murphy, L., Paul, F., Girard-Ardhuin, F., Chapron, B., Donlon, C.J., 2016. FluxEngine: a flexible processing system for calculating atmosphere–ocean carbon dioxide gas fluxes and climatologies. J. Atmos. Ocean. Technol. 33 (4), 741–756, http://dx.doi.org/10.1175/JTECH-D-14-00204.1.

StatSoft Inc., 2013. Electronic Statistical Textbook. StatSoft. WEB, Tulsa, OK, http://www.statsoft.com/textbook/.

Takahashi, T., Sutherland, S.C., Sweeney, C., Poisson, A., Metzl, N., Tilbrook, B., Bates, N., Wanninkhof, R., Feely, R.A., Sabine, C., Olafsson, J., Nojiri, Y., 2002. Global sea–air CO_2 flux based on climatological surface ocean pCO_2, and seasonal biological and temperature effects. Deep-Sea Res. Pt. II 49 (9–10), 1601–1622, http://dx.doi.org/10.1016/S0967-0645(02)00003-6.

Takahashi, T., Sutherland, S.C., Kozyr, A., 2008. Global Ocean Surface Water Partial Pressure of CO_2 Database: Measurements

Performed during 1968—2006 (Version 1.0). ORNL/CDIAC-152, NDP-088, Carbon Dioxide Information Analysis Center, Oak Ridge National Laboratory. U.S. Department of Energy, Oak Ridge, TN, p. 37831.

Takahashi, T., Sutherland, S.C., Wanninkhof, R., Sweeney, C., Feely, R.A., Chipman, D.W., Hales, B., Friederich, G., Chavez, F., Sabine, C., Watson, A., Bakker, D.C.E., Schuster, U., Metzl, N., Yoshikawa-Inoue, H.Y., Ishii, M., Midorikawa, T., Nojiri, Y., Köertzinger, A., Steinhoff, T., Hoppema, M., Olafsson, J., Arnarson, T. S., Tilbrook, B., Johannessen, T., Olsen, A., Bellerby, R., Wong, C. S., Delille, B., Bates, N.R., de Baar, H.J.W., 2009. Climatological mean and decadal change in surface ocean pCO_2 and net sea—air CO_2 flux over the global oceans. Deep-Sea Res. II 56 (8—10), 554—577, http://dx.doi.org/10.1016/j.dsr2.2008.12.009.

Telszewski, M., Chazottes, A., Schuster, U., Watson, A.J., Moulin, C., Bakker, D.C.E., González-Dávila, M., Johannessen, T., Körtzinger, A., Lüger, H., Olsen, A., Omar, A., Padin, X.A., Ríos, A.F., Steinhoff, T., Santana-Casiano, M., Wallace, D.W.R., Wanninkhof, R., 2009. Estimating the monthly pCO_2 distribution in the North Atlantic using a self-organizing neural network. Biogeosciences 6 (10), 1405—1421, http://dx.doi.org/10.5194/bg-6-1405-2009.

Thomas, H., Bozec, Y., Elkalay, K., de Baar, H.J.W., 2004. Enhanced open ocean storage of CO_2 from Shelf Sea pumping. Science 304 (5673), 1005—1008, http://dx.doi.org/10.1126/science.1095491.

Wanninkhof, R., McGillis, W.R., 1999. A cubic relationship between air—sea CO_2 exchange and wind speed. Geophys. Res. Lett. 26 (13), 1889—1892.

Wanninkhof, R., Asher, W.E., Ho, D.T., Sweeney, C.S., McGillis, W.R., 2009. Advances in quantifying air—sea gas exchange and environmental forcing. Ann. Rev. Mar. Sci. 1, 213—244, http://dx.doi.org/10.1146/annurev.marine.010908.163742.

Wanninkhof, R., Park, G.-H., Takahashi, T., Sweeney, C., Feely, R., Nojiri, Y., Gruber, N., Doney, S.C., McKinley, G.A., Lenton, A., Le Quéré, C., Heinze, C., Schwinger, J., Graven, H., Khatiwala, S., 2013. Global ocean carbon uptake: magnitude, variability and trends. Biogeosciences 10 (3), 1983—2000, http://dx.doi.org/10.5194/bg-10-1983-2013.

Weiss, R.F., Van Woy, F.A., Salameh, P.K., 1992. Surface Water and Atmospheric Gas Chromatography: Results From Expeditions Between 1977 and 1990. Scripps Institute of Oceanography. Carbon Dioxide Information Analysis, Centre Oak Ridge National Laboratory, NDP-044.

Woolf, D.K., Goddijn-Murphy, L.M., Prytherch, J., Yelland, M.J., Nightingale, P.D., Shutler, J.D., Piolle, J.-F., Hanafin, J., Chapron, B., 2013. Appropriate treatment of uncertainty and ambiguity; a flexible system for climatological calculations in response to an on-going debate on the transfer velocity. Proc. 'ESA Living Planet Symposium 2013', Edinburgh, 9—13 September 2013, 8 pp., http://www.oceanflux-ghg.org/content/download/75643/973537/file/Woolf_etal_LivingPlanet_2013.pdf.

Wrobel, I., Piskozub, J., 2016. Effect of gas-transfer-velocity parameterizations choice on air—sea CO_2 fluxes in the North Atlantic and the European Arctic. Ocean Sci. 12 (5), 1091—1103, http://dx.doi.org/10.5194/os-12-1091-2016.

Yasunaka, S., Murata, A., Watanabe, E., Chierici, M., Fransson, A., van Heuven, S., Hoppema, M., Ishii, M., Johannessen, T., Kosugi, N., Lauvset, S.V., Mathis, J.T., Nishino, S., Omar, A.M., Olsen, A., Sasano, D., Takahashi, T., Wanninkhof, R., 2016. Mapping of the air—sea CO_2 flux in the Arctic Ocean and its adjacent seas: basin-wide distribution and seasonal to interannual variability. Polar Sci. 10 (3), 323—334, http://dx.doi.org/10.1016/j.polar.2016.03.006.